Am J Cancer Res 2022;12(9):4211-4226
www.ajcr.us /ISSN:2156-6976/ajcr0142549

Original Article

Overexpression of transmembrane protein 102 implicates poor prognosis and chemoresistance in epithelial ovarian carcinoma patients

Yi-Jou Tai[1,2], Cheng-Miao Ou[3], Ying-Cheng Chiang[1], Chi-Fang Chang[1], Chi-An Chen[1], Wen-Fang Cheng[1,2,4]

[1]Department of Obstetrics and Gynecology, [2]Graduate Institute of Clinical Medicine, [3]Institute of Molecular Medicine, [4]Graduate Institute of Oncology, College of Medicine, National Taiwan University, Taipei, Taiwan

Received February 25, 2022; Accepted June 11, 2022; Epub September 15, 2022; Published September 30, 2022

Abstract: Most ovarian cancer patients experience disease recurrence and chemotherapeutic resistance, and the underlying mechanisms are unclear. Identifying relevant pathways could reveal new therapeutic targets. Here we examined expression of transmembrane protein 102 (TMEM102), a biomarker of prognosis and chemoresistance, in epithelial ovarian cancer (EOC), and assessed its role in inhibiting tumor cell apoptosis. We performed qRT-PCR to investigate the association of TMEM102 expression with clinical outcomes in 226 EOC patients. We also conducted *in vitro* studies to explore possible mechanisms through which TMEM102 may influence chemoresistance, including the effects of downregulating TMEM102 expression with small interfering RNA. Serous and high-grade carcinomas expressed significantly higher TMEM102 than normal ovarian tissues. TMEM102 was also overexpressed in patients with advanced-stage disease and chemoresistance. Reduction of TMEM102 expression by small interfering RNA induced ovarian cancer cell apoptosis after cytotoxic treatment. TMEM102 overexpression enhanced chemoresistance via upregulation of heat shock proteins 27, 60, and 70; and survivin, resulting in decreased cytochrome c in the mitochondria and decreased caspase 9 expression. Our results indicate that TMEM102 overexpression may promote chemoresistance via inhibition of a mitochondria-associated apoptotic pathway.

Keywords: TMEM102, apoptosis, epithelial ovarian carcinoma, chemoresistance

Introduction

Ovarian cancer is the seventh most common cancer among women in Taiwan, and is associated with high mortality and morbidity in Taiwan and in western countries [1-3]. A recent population-based study in Taiwan reported both increasing incidence and decreasing age at diagnosis [4]. Over 70% of patients are at an advanced stage when diagnosed with ovarian cancer. The main treatments include surgery and adjuvant platinum-based chemotherapy and/or targeted therapy [5, 6]. Recent trials show that maintenance therapy targeting VEGF and/or DNA repair defects improves long-term survival in selected patient groups [7-10]. However, 50-70% of patients experience disease relapse with metastasis, and develop resistance to chemotherapy, at which time treatment options are limited [11]. Several mechanisms of drug resistance in ovarian cancer have been proposed, including over-expression of multi-drug resistance genes, increased DNA repair, dysregulation of apoptosis, alterations of the tumor microenvironment, evasion of the host immune response, and enrichment of drug-resistant cancer stem cells [12-18]. Identifying the molecules and pathways involved in chemoresistance could open avenues to new treatment strategies.

TMEM102 is a transmembrane protein that has been identified as a proapoptotic molecule involved in GM-CSF deprivation-induced apoptosis [19]. TMEM102 also enhances T-cell adhesion and migration by chemokine-prompted T-cell trafficking and integrin-mediated cell adhesion [20, 21]. In addition to its proapoptotic function in primary hematopoietic cells, TMEM102 plays an oncogenic role in acute lymphoblastic leukemia cells through regulation of Akt-TSC2-mTORC1 signaling [22]. However, the

biological function of TMEM102 and its role in tumorigenesis in human epithelial cancers remains unclear.

Here, we investigated the correlation between TMEM102 expression and clinical outcomes in patients with epithelial ovarian carcinoma (EOC). We also performed *in vitro* studies to explore the possible involvement of TMEM102 in chemoresistance.

Materials and methods

Patients and specimens

For this study, we enrolled patients with EOC who received surgery and adjuvant platinum-based chemotherapy. All included patients provided informed consent before surgery, and the experimental protocols were approved by the Institutional Review Board of National Taiwan University Hospital. Tissue specimens were collected during surgery, immediately frozen in liquid nitrogen, and stored at -70°C until the experiments. As controls, normal ovarian tissue samples were collected from women undergoing surgery for benign gynecologic lesions, which were also immediately frozen in liquid nitrogen and stored at -70°C until the experiments. The maximal residual tumor size after surgery was recorded, and categorized as being ≤1 cm or >1 cm in size. Histological grading was based on the International Union Against Cancer criteria, and staging was based on the criteria of the International Federation of Gynecology and Obstetrics [23].

All patients received regular follow-up every 3 months after the primary treatment. Recurrence was defined as abnormal imaging results (computerized tomography or magnetic resonance imaging), elevated CA125 (over 2× the upper normal limit) on two consecutive tests with a 2-week interval, or biopsy-proven disease. Patients with disease progression or recurrence within 6 months after completing platinum-based chemotherapy were defined as chemoresistant, whereas patients without recurrence or relapse over 6 months after completion of initial chemotherapy were defined as chemosensitive. Progression-free survival (PFS) was defined as the period from completion of chemotherapy to the date of confirmed recurrence, disease progression, or last follow-up. Overall survival (OS) was defined as the period from surgery to the date of death from the disease, or the date of the last visit. From medical records, we collected clinical data, including age, clinical stage, surgical findings, treatment history, disease status, and survival. The detailed medical records were examined up to February 28, 2021.

RNA extraction from cancer tissues

From the tissue specimens, total RNA was isolated with Trizol reagent (Invitrogen Corporation, Carlsbad, CA, USA), following the manufacturer's instructions. The samples were subsequently passed through a Qiagen RNeasy column (Qiagen, Valencia, CA, USA) for removal of small fragments that could affect a reverse transcription reaction and hybridization quality. After RNA recovery, cDNA was synthesized using a chimeric oligonucleotide with an oligo-dT and a T7 RNA polymerase promoter, at a concentration of 100 pmol/μL.

Reverse-transcription polymerase chain reaction (RT-PCR)

First-strand cDNA was synthesized using a RevertAid first-strand cDNA synthesis kit (Thermo Fisher Scientific, Waltham, MA), and then qRT-PCR was performed using a LightCycler Real-Time detection system (Roche Diagnostics, Mannheim, Germany). The relative abundance of mRNA was calculated using the comparative method, with GAPDH as the internal control. TMEM102 was generated with 30 cycles using sense primer 5'-CAGGAATTGACCCAGCTGAT-3' and anti-sense primer 5'-CGTCACTAGGCGATTTTTCC-3'. GAPDH was generated with 30 cycles using sense primer 5'-ACCCAGAAGACTGTGGATGG-3' and antisense primer 5'-TGCTGTA GCCAAATTCGTTG-3'. The PCR products were analyzed in 1% agarose gel, with EtBr staining in TBE solution.

Real-time quantitative polymerase chain reaction (Real-time qPCR)

Real-time qPCR was conducted using the LightCycler Real-Time detection system (Roche Diagnostics, Mannheim, Germany). The relative abundance of mRNA was calculated using the comparative method with GAPDH as the internal control. GAPDH was detected using the primer Hs03929097_g1 (Applied Biosystems, Foster City, CA). TMEM102 was detected using

the primer Hs00401991_g1 (Thermo Fisher Scientific Inc., MA, USA).

We used the comparative $2^{-\Delta\Delta Ct}$ method to calculate the target gene expression, as previously described [24]. Quantitative data generation was based on the number of cycles required for the fluorescent signal to reach the threshold of detection (Ct value). The following equation was used to quantify the TMEM102 expression level of in each sample: relative expression level of TMEM102 = $2^{-\Delta\Delta Ct}$, $\Delta Ct = Ct_{target\ (TMEM102)} - Ct_{housekeeping\ (GAPDH)}$, $\Delta\Delta Ct = \Delta Ct_{sample\ (ovarian\ cancer\ tissue)} - \Delta Ct_{calibrator\ (normal\ ovarian\ tissue)}$.

Ovarian cancer cell lines

The human ovarian cancer cell lines SKOV3, OVCAR3, and ES2 were purchased from the American Type Culture Collection (Manassas, VA, USA). They were cultured in McCoy's 5A (modified) Medium (Thermo Fisher Scientific, Waltham, MA, USA) supplemented with 10% fetal bovine serum and 1% penicillin/streptomycin, and grown at 37°C with 5% CO_2. The CA5171 cell line, established in our lab, was cultured in RPMI-1640 supplemented with 20% fetal calf serum, 50 units/mL penicillin/streptomycin, 2 mM L-glutamine, 1 mM sodium pyruvate, and 2 mM nonessential amino acids, and grown at 37°C under 5% CO_2 [25]. The cells were rinsed with phosphate-buffered saline (PBS), detached using trypsin/EDTA, and then resuspended in fresh medium for subsequent experiments.

TMEM102 knock-down in SKOV3 and CA5171 cells

SKOV3 and CA5171 cells were cultured in 6-well plates to 50-60% confluence. Next, Lipofectamine RNAi Max (Invitrogen #1875252), and either scrambled siRNA (OriGene SR300-04) or TMEM102 siRNA (OriGene SR317107), were added following the manufacturers' instructions. The siGAPDH (Invitrogen, Carlsbad, CA, USA) was used as control siRNA. After transfection of SKOV3 and CA5171 cells with TMEM102 siRNA (si-TMEM102), the *in vitro* knock-down of TMEM102 expression was assessed by RT-PCR analyses. Briefly, SKOV3 and CA5171 cells were grown in 6-cm dishes, and transiently transfected with 50 pmol siRNA using 8 μg TransFast™ transfection reagent (Promega, Madison, WI, USA) in a total transfection volume of 2 mL serum-free RPMI-1640 medium. After incubation, RPMI-1640 medium containing 20% normal growth media was added. Various transfectants (e.g., SKOV3 si-TMEM102 and CA5171 si-TMEM102) were analyzed for further experiments.

Transfection of ES2 cells with TMEM102

To generate pcDNA3.1-TMEM102, TMEM102 was first amplified by PCR using human placenta cDNA as the template, and the primer set 5'-CCGG TCTAGA ATGGCTTCCGCAGTCTG-GGG-3' and 5'-CGCGGATCCTTAATGGGCCCCG-CCCCCCA-3'. Next, the amplified product was cloned into the XbaI/BamHI sites of the pcDNA3.1 vector (Invitrogen, Carlsbad, CA, USA). TMEM102 was transfected into ES2 using LipofectAMINE reagent (Life Technologies, Paisley, UK) following the manufacturer's instructions. To select the TMEM102-overexpressing ES2 transfectants (ES2-TMEM102), neomycin was added to the culture medium after transfection. The neomycin-resistant clones were individually picked, expanded, and assayed by RT-PCR for expression of the transfected TMEM102. The subsequent experiments were performed using original ES2 and TMEM102-overexpressing ES2 transfectants (ES2-TMEM102).

Apoptotic assay of ovarian cancer cells treated with various cytotoxic drugs

We harvested parental SKOV3, CA5171, and ES2 cells; mock-transfected cells of each type; and SKOV3 si-TMEM102, CA5171 si-TMEM102 cells, and ES2-TMEM102 cells. All were incubated overnight in serum-free medium and treated for 24 or 48 hours with a cytotoxic agent (Sigma-Aldrich, St. Louis, MO, USA), i.e., paclitaxel (1.5 μM), cisplatin (12.5 μM), doxorubicin (0.3 μM), or topotecan (0.1 μM). Drugs were prepared according to the manufacturer's instructions. Cells treated with PBS were used as negative control. Tumor cells and their transfectants, including adherent and floating cells, were collected and incubated with annexin V and 7-amino-actinomycin D (7-AAD) (BD Biosciences, Franklin Lakes, NJ, USA) for flow cytometry (FACScan; BD Biosciences). Apoptosis was quantified based on the percentage of the population shifting to fluorescein positivity.

Immunoblotting for apoptosis-related proteins

To detect apoptotic proteins involved in TMEM102-mediated anti-apoptosis, we used the Human Apoptosis Antibody Array (R&D Systems, Minneapolis, MN, USA). For this purpose, we isolated total cell extracts from original ES2 cells and the mock and TMEM102 transfectants (ES2-TMEM102) after paclitaxel treatment, and subjected them to apoptosis array analysis following the manufacturer's instructions. Briefly, protein samples were incubated with each array overnight at 4°C on a rocking platform shaker. After removal of unbound proteins, the arrays were washed with washing buffer, then incubated with the primary antibody solution for 2 hours at room temperature, and then washed again with washing buffer. Next, secondary antibody solution was added to the arrays, followed by incubation for 1 hour on a rocking platform shaker. The arrays were then washed three times with washing buffer, and protein spots were visualized using the chemiluminescence detection reagents supplied in the array kits. The produced signal is proportional to the amount of bound analyte. For each duplicated array spot, the intensity score was measured with ImageJ (1.53v, National Institutes of Health) software, and the average intensity was calculated by subtracting the averaged background signal. The fold change was determined by comparing the incremental change in apoptotic proteins after cytotoxic agent treatment in TMEM102-transfected ES2 cells with that in mock transfected cells (indicated as a value of 1).

Western blot analysis to verify the result of the apoptosis array

After the original ES2 cells and the mock and TMEM102 transfectants were treated with cytotoxic agents, the cells were lysed in immunoprecipitation assay buffer, and the protein extracts were quantified using the BCA Protein Assay Kit (Pierce, Rockford, IL, USA). The cell lysates (50 μg) were resolved on a sodium dodecyl sulfate-containing 12% polyacrylamide gel, transferred to polyvinylidene difluoride nylon membranes (Millipore, Bedford, MA, USA), and probed with specific antibodies against GAPDH (ab8245; abcam), TMEM102 (PA5-55077; dilution 1:500; Thermo Fisher Scientific), cytochrome c (4272; dilution 1:1000; Cell Signaling), APAF1 (8969; dilution 1:1000; Cell Signaling), caspase 9 (9508; dilution 1:1000; Cell Signaling), caspase 3 (9662; dilution 1:1000; Cell Signaling), and PARP (9542; dilution 1:1000; Cell Signaling). Next, the membrane was probed with HRP-conjugated secondary antibody. The specific bands were visualized using an ECL™ Western blot system (GE Healthcare, Little Chalfont, UK).

Protein levels were quantified by densitometric analysis, and normalized to the GAPDH levels (control) using ImageJ (version 1.53; National Institutes of Health) and Prism (version 9; GraphPad) software. The expression level of each protein was presented as the fold change compared with the density of GAPDH, and the expression levels in the original ES2 cells were used as reference.

Statistical analysis

Data were analyzed using SPSS version 17.0 (SPSS Inc., Chicago, IL, USA). Comparisons between unpaired groups were made using one-way analysis of variance (ANOVA) or the Mann-Whitney U test for continuous variables, and Fisher's exact test for categorical variables. The median mRNA expression level was used as the cut-off value to categorize patients as low or high TMEM102 expression for further analysis. TMEM102 levels ≥0.04 were defined as high TMEM102 expression, and those <0.04 were defined as low TMEM102 expression. Survival analysis was performed using Kaplan-Meier plots and the log-rank test to calculate differences in survival curves. Cox regression analysis was used to evaluate prognostic factors for recurrence and death. All data are expressed as the mean ± standard error from at least three experiments. A *P*-value of <0.05 was considered statistically significant.

Results

TMEM102 expression is higher in EOC tissue than in benign ovarian tumors and normal ovaries

Of the 264 women enrolled in this study, 226 had EOC, 26 had benign ovarian tumors, and 12 were menopausal women with atrophic ovaries. We performed qRT-PCR to evaluate the TMEM102 mRNA expression levels, with GAPDH used as the reference gene. Mean

TMEM102 expression levels were higher in cancerous tissues (0.125) than in benign ovarian lesions (0.016) and normal ovaries (0.015) (P<0.001, Mann-Whitney U; **Figure 1A**). TMEM102 expression was further validated by RT-PCR and western blot analysis (**Figure 1B**), and the protein expression levels were significantly higher in ovarian cancerous tissues than in noncancerous tissues.

Clinicopathological characteristics of patients with EOC

Table 1 shows the relevant characteristics of the patients with EOC. The mean age at diagnosis was 53.4 years, 28.8% (65/226) had early-stage disease, and 71.2% (161/226) had advanced-stage disease. Serous histology accounted for 50% (113/226), clear cell 32.3% (73/226), endometrioid 16.4% (37/226), and carcinosarcoma 1.3% (3/226). High-grade tumors (grade 3) accounted for 78.8% (178/226). After primary surgery, 37.6% (85/226) of the patients had residual tumors larger than 1 cm. The disease was platinum-sensitive in 161 women (71.2%), and platinum-resistant in 65 (28.8%). Disease recurrence or progression occurred in 148 patients (65.5%), and 76 (33.6%) died of the disease. The median PFS was 21 months (2-60 months) and median OS was 48 months (3-60 months).

TMEM102 expression correlates with the clinicopathological characteristics of patients with EOC

We further investigated correlations between TMEM102 expression (assessed using qRT-PCR) and various clinicopathological characteristics (**Figure 1C**). Mean TMEM102 expression levels were higher in patients with high-grade tumors (0.057 vs. 0.023, P=0.005), advanced-staged disease (0.046 vs. 0.023, P=0.014), chemoresistance (0.057 vs. 0.034, P=0.022), recurrence (0.054 vs. 0.016, P=0.012), and poor outcome (0.053 vs. 0.034, P=0.045) compared with corresponding controls (all by Mann-Whitney U test) (Supplementary Table 1).

TMEM102 expression correlates with PFS and OS

We further evaluated whether TMEM102 expression correlated with the survival of patients with ovarian cancer (**Figure 2**). Compared to patients with low TMEM102 expression (<0.04), patients with high TMEM102 expression (≥0.04) had a shorter PFS (log-rank test, P<0.001) and OS (log-rank test, P=0.004) (**Figure 2A**). We further analyzed survival among 141 patients with a residual tumor diameter of ≤1 cm (optimal surgery) after primary debulking surgery. In this patient group, those with high TMEM102 expression (≥0.04) had shorter PFS (log-rank test, P=0.006) and OS (log-rank test, P=0.054) (**Figure 2B**). Among 161 patients with advanced-stage disease, those with high TMEM102 expression (≥0.04) still had shorter PFS (log-rank test, P=0.038) but OS did not significantly differ compared to patients with low TMEM102 expression (<0.04) (**Figure 2C**).

Using Cox regression analysis, we evaluated hazard ratios (HRs) and 95% confidence intervals (CIs) for various risk factors related to recurrence and death among the 226 patients with EOC. As shown in **Table 2**, univariate analysis revealed the following risk factors for disease recurrence: advanced stage (HR 5.12, 95% CI: 3.11-8.43, P<0.001), serous histology (HR 1.94, 95% CI: 1.39-2.72, P<0.001), high grade (HR 2.32, 95% CI: 1.46-3.69, P<0.001), residual tumor size larger than 1 cm after surgery (HR 2.70, 95% CI: 1.92-3.70, P<0.001), and high TMEM102 expression (≥0.04) (HR 1.73, 95% CI: 1.24-2.44, P=0.001). Upon multivariate analysis, three independent risk factors remained: advanced stage (HR 4.03, 95% CI: 1.11-14.62, P=0.03), residual tumor diameter larger than 1 cm after surgery (HR 1.56, 95% CI: 1.02-2.38, P=0.04), and high TMEM102 expression (≥0.04) (HR 1.70, 95% CI: 1.11-2.59, P=0.013).

Univariate analysis revealed the following risk factors for disease-related death: advanced stage (HR 5.53, 95% CI: 2.50-12.2, P<0.001), residual tumor diameter larger than 1 cm after surgery (HR 3.33, 95% CI: 2.08-5.26, P<0.001), and high TMEM102 expression (HR 1.63, 95% CI: 1.02-2.60, P<0.04). Multivariate analysis showed only two independent risk factors: advanced stage (HR 11.2, 95% CI: 2.42-51.8, P=0.002) and residual tumor diameter larger than 1 cm (HR 2.17, 95% CI: 1.25-3.85, P=0.011). High TMEM102 expression was no longer a statistically significant risk factor after adjusting for disease stage and residual tumor size.

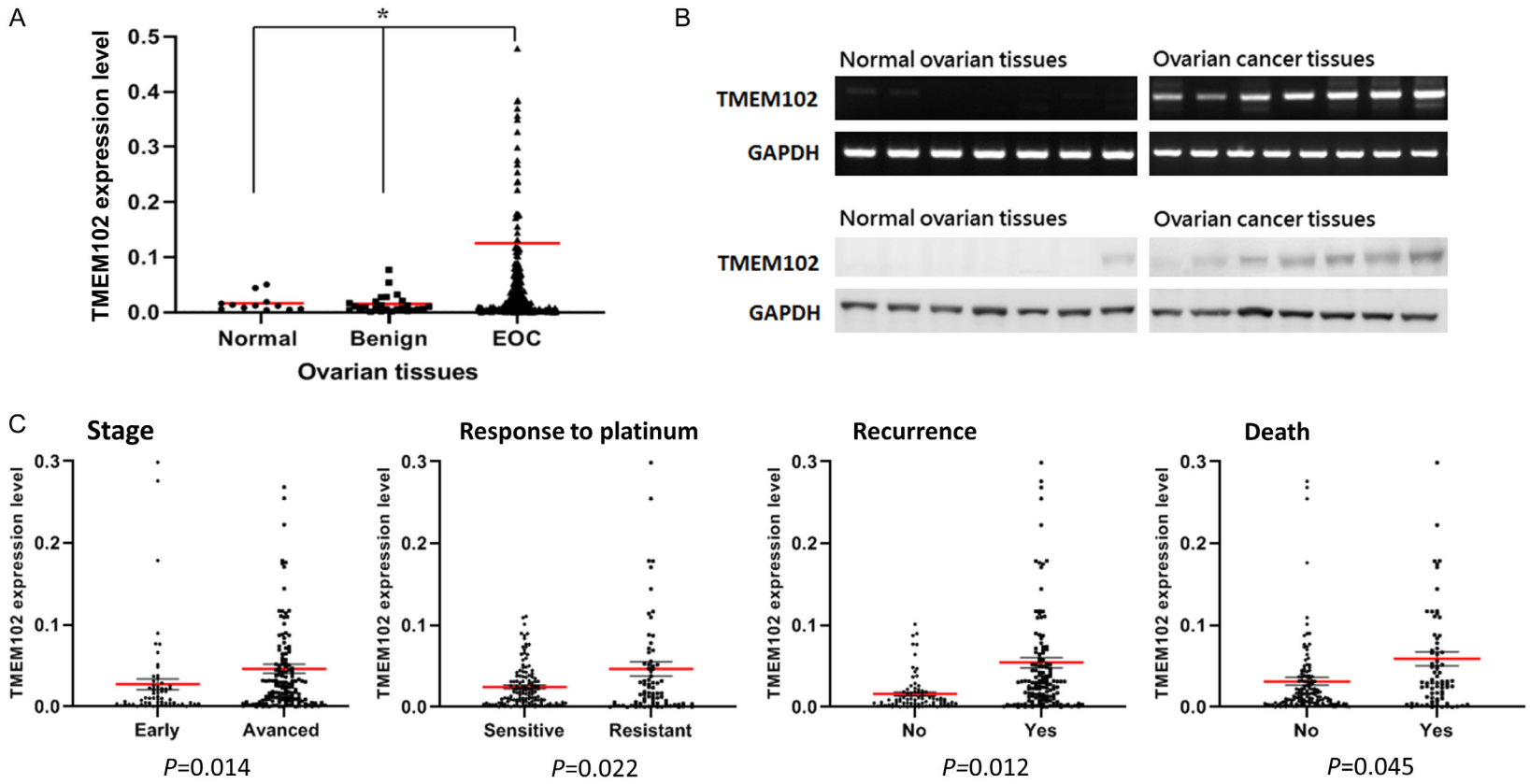

Figure 1. TMEM102 expression in various ovarian tissues. A. TMEM102 mRNA expression levels in normal ovaries, benign ovarian tumors, and epithelial ovarian cancer tissues (*P<0.05, Kruskal-Wallis). B. RT-PCR of TMEM102 mRNA expression (upper panels) and western blotting of TMEM102 protein expression (lower panels) in normal ovaries, and ovarian cancer tissues. C. Mean TMEM102 mRNA expression levels of the 226 patients and subgroup analysis (*P*-value by Mann-Whitney U test).

Table 1. Clinicopathologic characteristics and treatment outcomes of the 226 women with EOC

	Number	Percentage (%)
Total patients	226	100
Age (years)	53.4 ± 1.2	
FIGO stage		
Early (I, II)	65	28.8
Advanced (III, IV)	161	71.2
Histology		
Serous	113	50.0
Endometrioid	37	16.4
Clear cell	73	32.3
Carcinosarcoma	3	1.3
Tumor grade		
Low (I/II)	48	21.2
High (III)*	178	78.8
Post-operative residual tumor size		
≤1 cm	141	62.4
>1 cm	85	37.6
Chemotherapy response†		
Platinum-sensitive	161	71.2
Platinum-resistant	65	28.8
Treatment outcome		
Recurrence and/or progression	148	65.5
Death	76	33.6
Progression-free survival (months) (median, range)	21 (2-60)	
Overall survival (months) (median, range)	48 (3-60)	

*Clear cell carcinoma and carcinosarcoma (mixed Müllerian tumor) were defined as high-grade tumors. †Platinum-resistant was defined as showing relapse or progression within 6 months of platinum-off treatment.

TMEM102 inhibits apoptosis of human ovarian cells treated with cytotoxic drugs

We first evaluated TMEM102 protein expression in various human ovarian cancer cell lines. The TMEM102 protein expression levels were higher in SKOV3, OVCAR3, and CA5171 cells compared to in ES2 cells (**Figure 3A1**). We generated TMEM102-knockdown cells (SKOV3 si-TMEM102 and CA5171 si-TMEM102) and TMEM102-transfected ES2 cells (ES2-TMEM-102) for *in vitro* apoptosis-related assays. The TMEM102 RNA transcription levels were lower in various SKOV3 si-TMEM102 transfectants compared to in the mock-transfected and original SKOV3 cells (**Figure 3A2**). The TMEM102 RNA transcription levels were higher in various ES2 TMEM102 transfectants compared to in the mock-transfected and original ES2 cells (**Figure 3A2**).

We used flow cytometry to further evaluate the chemoresponse of various parental ovarian cancer cell lines and their transfectants. In **Figure 3B**, a flow cytometric dot plot shows the representative results for the detection of annexin V-positive and 7AAD-positive SKOV3 parental cells and their TMEM102 transfectants treated with doxorubicin. After paclitaxel treatment for 24 hours, the incremental fluorescence intensities for annexin V^+7AAD^+ cells were higher for CA5171 si-TMEM102 transfectants (12.85±3.94) compared to the parental CA5171 cells (8.8±0.06) and mock-transfected CA5171 cells (4.96±0.30) (P=0.016, ANOVA; **Figure 3C**). After treatment with doxorubicin for 24 hours, the incremental fluorescence intensities of annexin V^+7AAD^+ cells were also higher for CA5171 si-TMEM102 transfectants (15.0±2.18) compared to the parental CA5-171 cells (6.04±0.21) and mock-transfected CA5171 cells (3.34±0.73) (P<0.0001, ANOVA). Similarly, after 48 hours of topotecan treatment, the incremental fluorescence intensities of annexin V^+7AAD^+ cells were higher for the CA5171 si-TMEM102 transfectants (29.63±

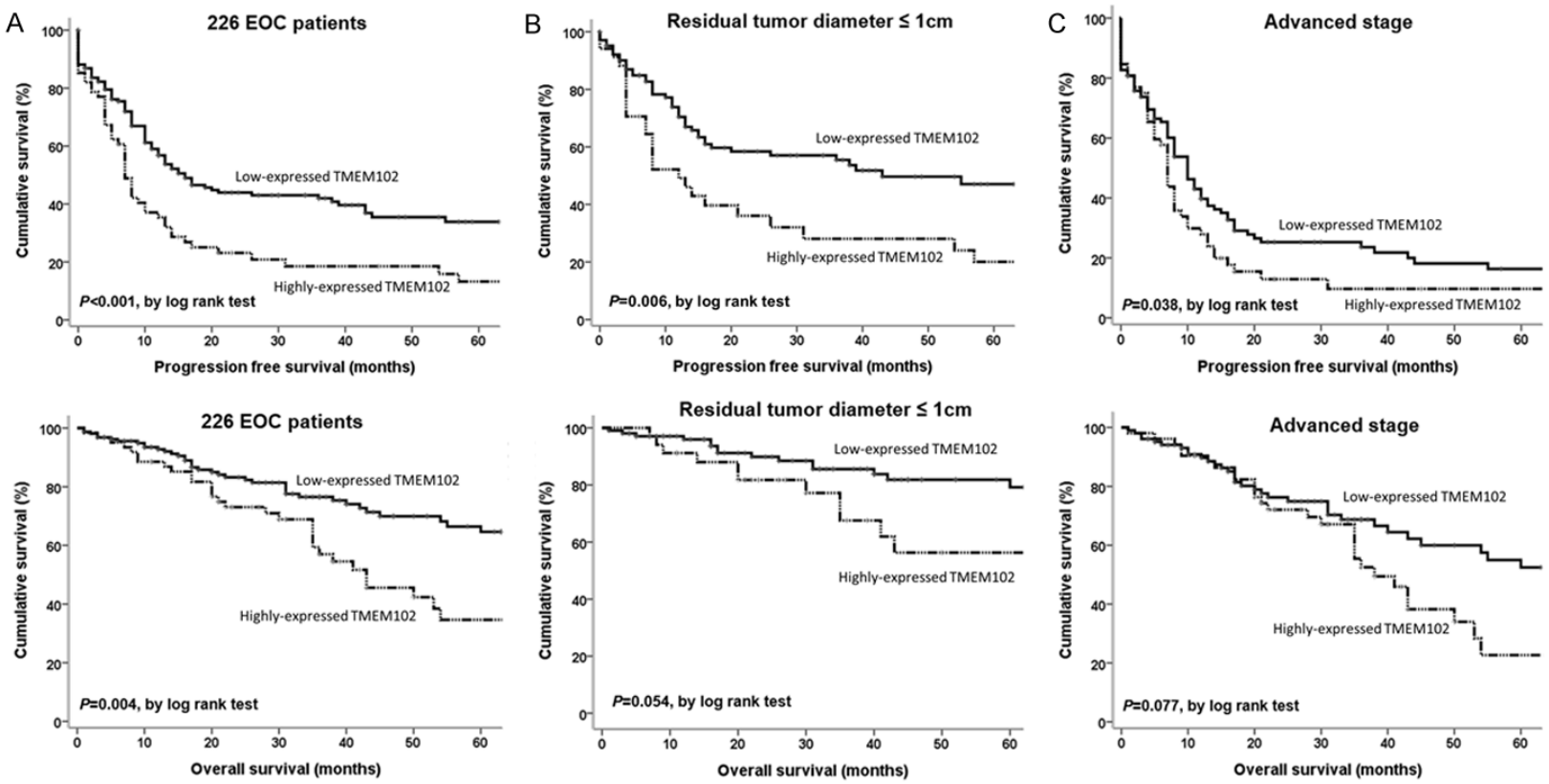

Figure 2. Correlations of TMEM102 expression with progression-free survival (PFS) and overall survival (OS) among patients with epithelial ovarian carcinoma. A. Patients with tumors showing high TMEM102 expression had shorter PFS (P<0.001) and shorter OS (P=0.004). B. Survival of 141 patients who underwent optimal debulking surgery with residual tumor diameter ≤1 cm. Patients whose tumors showed high TMEM102 expression had shorter PFS (P=0.006) and OS (P=0.054). C. Among 161 patients with advanced disease (stage III and IV), those whose tumors exhibited high TMEM102 expression had shorter PFS (P=0.038). All differences were calculated using the log-rank test.

Table 2. Cox regression analysis of risk factors for recurrence and death

	Numbers	Recurrence				Death			
		Univariate		Multivariate		Univariate		Multivariate	
		HR (95% CI)	P	HR (95% CI)	P	HR (95% CI)	P	HR (95% CI)	P
FIGO stage									
Early	65	1		1		1		1	
Advanced	161	5.12 (3.11-8.43)	<0.001	4.03 (1.11-14.62)	0.033	5.53 (2.50-12.2)	<0.001	11.2 (2.42-51.8)	0.002
Histology									
Non-serous	113	1		1		1			
Serous	113	1.94 (1.39-2.72)	<0.001	1.20 (0.62-2.34)	0.064	1.23 (0.78-1.95)	0.37		
Tumor grade									
Low (I/II)	48	1		1		1			
High (III)	178	2.32 (1.46-3.69)	<0.001	1.23 (0.71-2.12)	0.46	1.28 (0.71-2.31)	0.41		
Post-operative residual tumor size									
≤1 cm	141	1		1		1		1	
>1 cm	85	2.70 (1.92-3.70)	<0.001	1.56 (1.02-2.38)	0.042	3.33 (2.08-5.26)	<0.001	2.17 (1.25-3.85)	0.011
Platinum-based chemotherapy									
Without paclitaxel	55	1		1	0.804	1			
With paclitaxel	171	2.36 (1.32-4.21)	0.004	1.11 (0.50-2.49)		2.30 (1.01-5.22)	0.054		
TMEM102 expression*									
Low (<0.04)	167	1		1		1		1	
High (≥0.04)	59	1.73 (1.24-2.44)	0.001	1.70 (1.11-2.59)	0.013	1.63 (1.02-2.60)	0.044	1.54 (0.99-2.58)	0.052

HR: hazard ratio; CI: confidence interval. *The median TMEM102 mRNA expression level was used as the cut-off value.

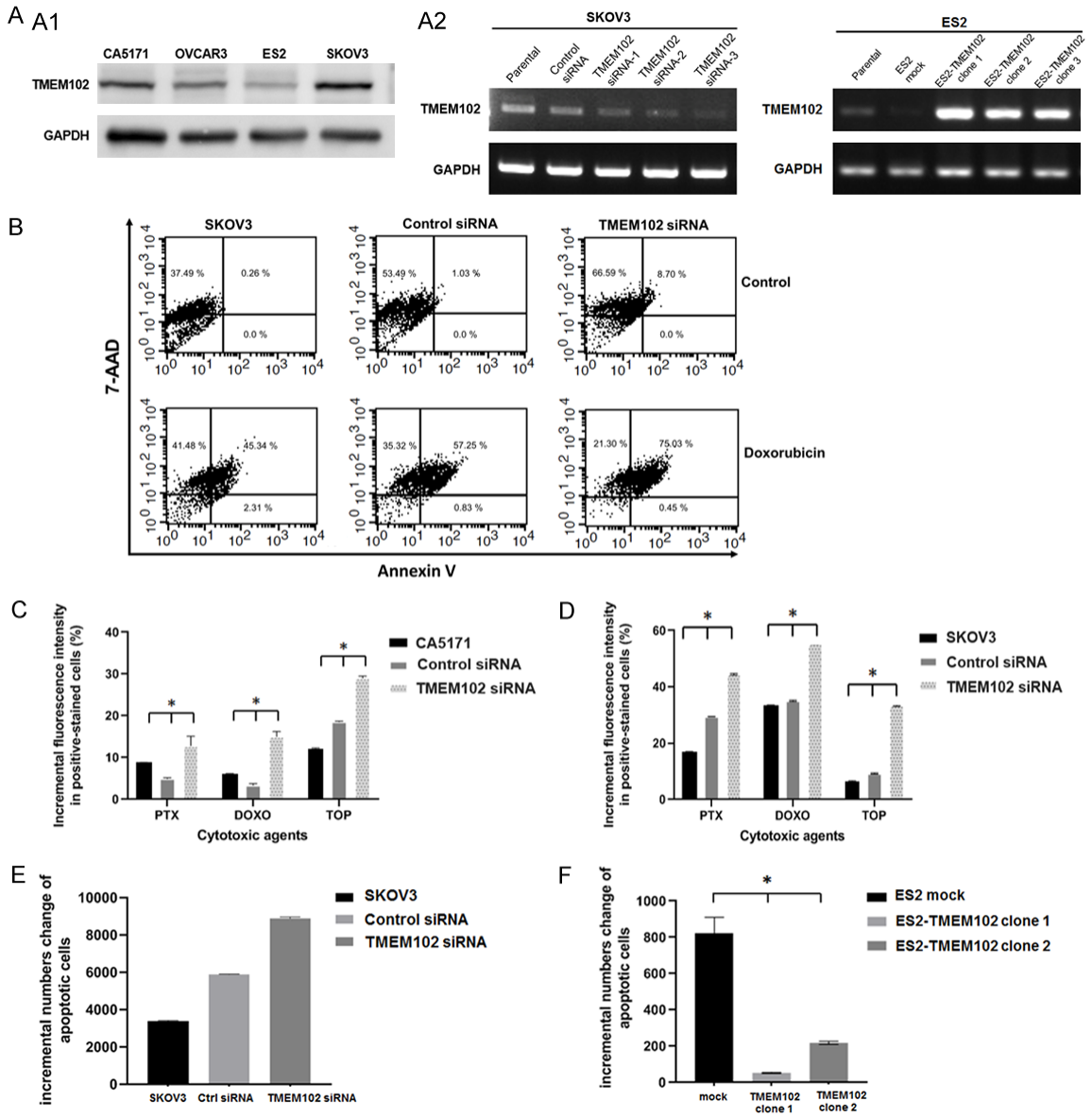

Figure 3. I*n vitro* apoptotic assays of various ovarian cancer cells and their transfectants after treatment with various cytotoxic drugs. A. A1: Western blot showing TMEM102 protein expression in various ovarian cancer cell lines. A2: RT-PCR results for TMEM102 expression in ovarian cancer cell lines. TMEM102 expression was lower in SKOV3 si-TMEM102 transfectants compared to in SKOV3 original cells and mock-transfectants. TMEM102 expression was higher in ES2-TMEM102 transfectants than in original ES2 cells and mock transfectants. B. Representative image showing flow cytometric analysis for annexin V and 7AAD staining in SKOV3 original cells and transfectants treated with doxorubicin. The percent of cells at the indicated times is shown in quadrant plots. C. Bar graphs showing the incremental fluorescence intensity of annexin V-positive and 7AAD-positive cells among CA5171 original cells and transfectants treated with paclitaxel (PTX), doxorubicin (Doxo), or topotecan (Top) (*P<0.05, ANOVA). D. Bar graphs of the incremental fluorescence intensity of annexin V-positive and 7AAD-positive cells among SKOV3 original cells and transfectants treated with paclitaxel (PTX), doxorubicin (Doxo), or topotecan (Top) (*P<0.05, ANOVA). E. Bar graphs showing the incremental changes of apoptotic cell numbers among SKOV3 original cells and transfectants treated with paclitaxel for 48 hours. F. Bar graphs showing the incremental changes or apoptotic cell numbers among ES2 original cells and transfectants treated with paclitaxel for 24 hours (*P<0.05, ANOVA).

0.88) compared to parental CA5171 cells (12.17±0.27) and mock-transfected CA5171 cells (18.54±0.31) (P<0.0001, ANOVA).

As shown in **Figure 3D**, after treatment with a cytotoxic agent, the percentage of apoptotic cells was significantly higher among SKOV3 si-

TMEM102 transfectants compared with in parental and mock-transfected SKOV3 cells. Additionally, TMEM102 knockdown significantly increased the number of apoptotic cells after paclitaxel treatment: 8896±108.1 in SKOV3 si-TMEM102 vs. 3373±79.4 in parental SKOV3, and 5889±31.9 in mock transfected SKOV3 ($P<0.0001$, ANOVA; **Figure 3E**). In contrast, TMEM102 overexpression inhibited apoptosis, as manifested by the decreased incremental change in apoptotic cell numbers after paclitaxel treatment: 54±6 in ES2-TMEM102 clone 1, and 219±15.3 in ES2-TMEM102 clone 2 vs. 825±149.1 in ES2-mock ($P<0.0001$, ANOVA; **Figure 3F**). Taken together, these results suggested that TMEM102 confers resistance to the cytotoxic drug-induced apoptosis of human ovarian cancer cells.

TMEM102 involves the mitochondrial pathway of apoptosis

We further evaluated whether TMEM102 might inhibit apoptosis by regulating apoptosis-related molecules. We first investigated the relative changes in the expressions of 35 apoptosis-related proteins using Proteome Profiler™ Antibody Arrays (**Figure 4A**). As shown in **Figure 4B**, TMEM102 significantly upregulated the levels of anti-apoptotic molecules, including Bcl-2 antagonist of cell death (Bad) ($P<0.001$), heat shock protein (HSP) 27 ($P=0.0014$), HSP60 ($P=0.0012$), HSP70 ($P=0.006$), and survivin ($P=0.046$). Conversely, TMEM102 downregulated the level of the apoptotic protein cytochrome c ($P=0.0009$, Mann-Whitney U; **Figure 4B**). We found no differences in the levels of pro-caspase-3, cleaved caspase-3, Bax, or Bcl-2.

We next examined the expressions of various apoptosis-related molecules by immunoblotting (**Figure 4C**). Compared to mock-transfected ES2 cells, the ES2 TMEM102 transfectants exhibited significantly decreased expressions of cytochrome c ($P=0.014$), caspase 9 ($P=0.0003$), and PARP ($P<0.001$) (ANOVA; **Figure 4D**). We found no differences in the protein levels of APAF1 or caspase 3. Taken together, these results indicated that TMEM102 may act via a mitochondrial pathway to inhibit apoptosis.

Discussion

TMEM102, also known as GM-CSF/IL-3/IL-5 receptor common beta-chain-associated protein, is encoded by the *TMEM102* gene. The common β-chain (βc) is shared by the GM-CSF (granulocyte-macrophage colony-stimulating factor), interleukin (IL)-3, and IL-5 receptors. The βc-subunit is the principal signal-transducing subunit of the receptors after cytokine binding. Activation of the receptors initiates multiple signaling pathways that regulate cell proliferation and cell survival, including the Janus kinase 2 (JAK2)/activator of transcription (STAT), mitogen-activated protein kinase (MAPK), and PI3K/Akt pathways [26]. Mutation of βc disrupts the binding of GM-CSF, IL-3, and IL-5, and antibodies specific for the βc site block the functions of all three [27, 28]. These findings have important implications regarding new treatments of hematological malignancies and inflammatory diseases. Kao *et al*. found that the association of βc with TMEM102, and overexpression of TMEM102, induces activation of caspases 3, 8, and 9 and the pro-apoptotic molecules Bak and Bax in cytokine-dependent leukemic cell lines [19]. An oncogenic contribution of TMEM102, through the activation of mTORC1 signaling, was first reported in leukemia [22], but the exact role of TMEM102 in carcinoma is unclear.

In this study, we first observed that TMEM102 protein expression was higher in tissues from ovarian carcinoma than in normal ovaries or benign ovarian tumors. To assess the clinicopathological importance of TMEM102 expression in ovarian cancer tissues, we used qRT-PCR to quantitatively measure TMEM102 expression. We found that TMEM102 expression had prognostic significance in EOC, and was higher in patients with serous histological type, advanced stage, and chemoresistant disease. High TMEM102 expression was associated with recurrence and poor survival, even among patients with small or no residual tumor. Multivariate Cox regression analysis of survival indicated that only advanced stage, postoperative residual tumor larger than 1 cm, and high TMEM102 expression were independent risk factors for recurrence. However, high TMEM102 expression no longer exhibited a significant effect on overall survival after adjustment for disease stage and residual tumor size. It is well known that stage at diagnosis is the major determinant of survival in ovarian cancer, and complete resection of all macroscopic disease is the most important independent prognostic factor in advanced ovarian cancer [29, 30]. The lack of OS benefit might be explained by small

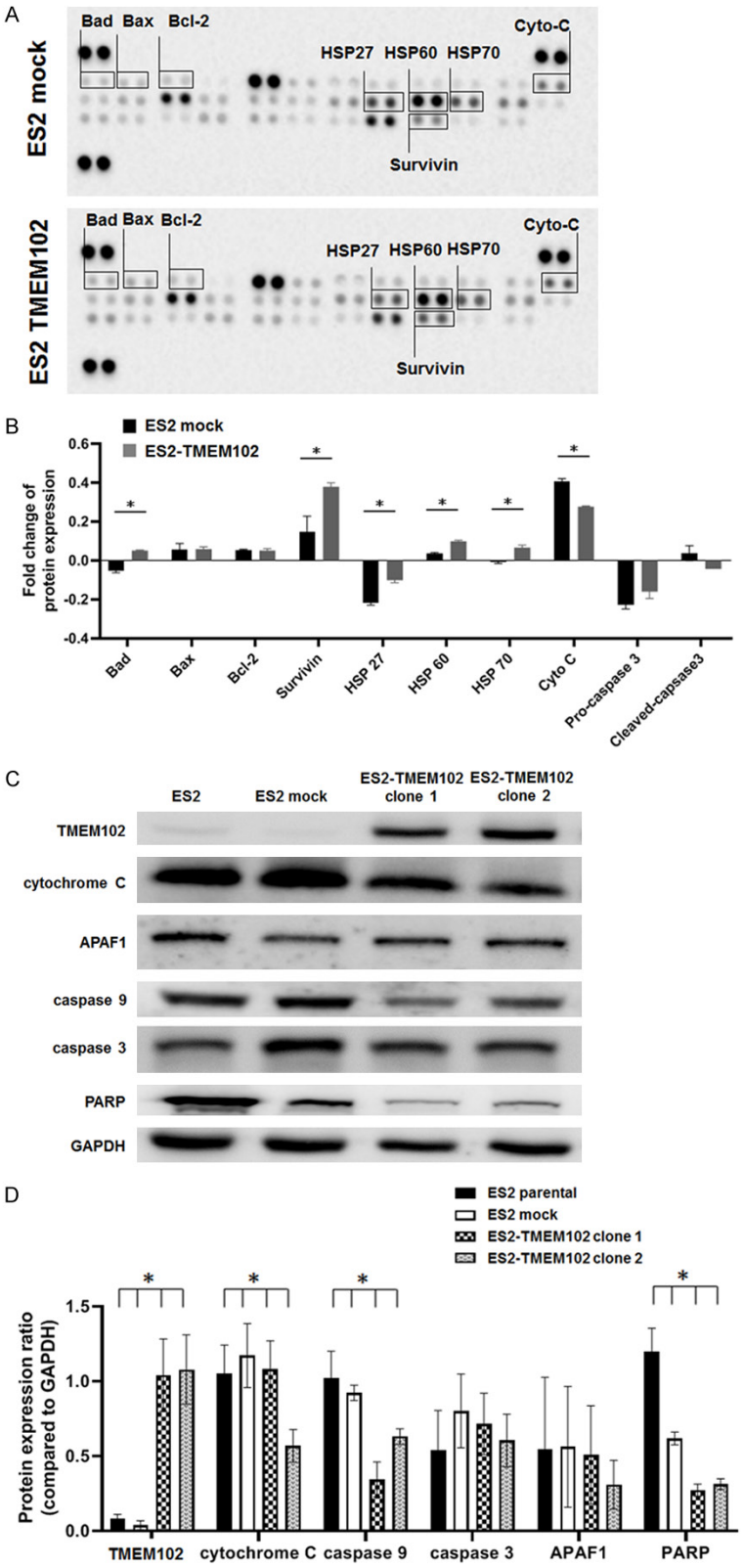

Figure 4. Analysis of various apoptosis-associated proteins in ES2 original cells and transfectants. A. Representative expression levels of various apoptosis-related proteins in ES2 mock-transfected cells and ES2 transfectants treated with paclitaxel. Rectangles indicate upregulated or downregulated proteins on the apoptosis arrays. B. Differentially expressed protein levels presented as histograms with statistical differences. Data are mean ± standard error (n=3 per group). *P<0.05, Mann-Whitney U. C. Western blot analysis of ES2 original cells and transfectants. D. Bar graphs of protein expression of various molecules in ES2 original cells and transfectants. TMEM102-transfected ES2 cells showed significantly decreased expressions of cytochrome c (original ES2: 1.05±0.19; ES2 mock: 1.17±0.21; ES2-TMEM102 clone 1: 1.08±0.19; ES2-TMEM102 clone 2: 0.57±0.11), caspase 9 (original ES2: 1.02±0.18; ES2 mock: 0.92±0.05; ES2-TMEM102 clone 1: 0.34±0.12; ES2-TMEM102 clone 2: 0.63±0.05), and PARP (original ES2: 1.20±0.15; ES2 mock: 0.62±0.04; ES2-TMEM102 clone 1: 0.27±0.04; ES2-TMEM102 clone 2: 0.31±0.03) (*P<0.05, ANOVA).

patient numbers, the use of salvage therapy after tumor progression, the fact that the TMEM102 cut-off value was not defined by an outcome-oriented approach, and the possible bias in the process of categorizing continuous data. Another possible explanation is that TMEM102 expression is not a major prognostic factor itself, but rather a predictive surrogate for tumor aggressiveness that overlaps with disease stage and residual tumor status.

We hypothesized that ovarian cancer tumors with high TMEM102 expression could develop resistance to chemotherapy, resulting in disease progression. To test this hypothesis, we subjected various ovarian cancer cell lines to treatment with cytotoxic agents (paclitaxel, cisplatin, doxorubicin, or topotecan). We observed a markedly increased percentage of apoptotic cells in ovarian cancer cell lines with siRNA-mediated TM-

EM102 downregulation compared to cells transfected with control siRNA. Furthermore, TMEM102 overexpression reduced the percentage of apoptotic cells, and led to resistance to cytotoxic treatments.

Despite evolving treatments and radical surgical techniques for EOC, resistance to chemotherapeutic agents has remained challenging. Cancer cells develop resistance via distinct mechanisms, including altered drug targets and signaling transduction molecules, increased repair of drug-induced DNA damage, and deregulation of apoptosis [31]. In this study, we demonstrated that TMEM102 overexpression induced chemoresistance, and that this effect was not restricted to a single agent, which implies that evasion of apoptosis is the mechanism of resistance. We conducted apoptosis-associated proteins blot array analysis, which revealed increased levels of Bad, survivin, and several HSPs (including HSP27, HSP60, and HSP70) in TMEM102-transfected ovarian cancer cells after paclitaxel treatment. Bad regulates apoptosis by interaction with Bcl-2 proteins, which function to maintain the integrity of outer mitochondrial membranes [32, 33]. Some studies show that Bad expression and phosphorylation status influence the chemosensitivity of cancer cells [34-36]. However, in our study, changes in Bad proteins did not correlate with changes in Bax or Bcl-2 proteins in TMEM102-overexpressing ovarian cancer cells following paclitaxel treatment. Drug resistance is a multifactorial process, and accumulating evidence shows that cancer stem cell signatures promote proliferation, invasion, epithelial-mesenchymal transition, and angiogenesis [37]. We found that TMEM102-overexpressing ES2 cells did not exhibit increased invasion activity, but showed a significantly increased proliferation rate (Supplementary Figure 1). Our findings revealed that TMEM102 had multiple roles in ovarian cancer cells, including involvement in chemo-resistance and proliferation.

Survivin is part of the inhibitor of apoptosis (IAP) family, members of which are overexpressed in many cancers, including ovarian cancer [38-40]. Survivin antagonizes mitochondria-dependent apoptosis associated with cytochrome c, caspase 7, caspase 9, and Smac/DIABLO [41, 42]. In agreement with earlier studies, here we observed survivin upregulation in TMEM102-overexpressing ovarian cancer cells. Another key finding of our study was alterations of HSPs. Some groups have found that HSPs play essential roles in regulating apoptosis and cell death [43]. Reports have highlighted HSP27 as an antagonist of caspases 3 and 9, and an inhibitor of cytochrome c and Smac/DIABLO release from the mitochondria [44]. HSP27 may suppress other apoptotic death receptor pathways, including tumor necrosis factor α, Fas, and TRAIL [45]. Other HSPs are involved in ovarian cancer resistance through positive regulation of survivin and Bcl-2 expression, which promotes cell survival [46]. Increased cytosolic HSP expression is associated with tumor progression and chemoresistance in various cancers [47, 48]. Besides their intracellular localization (including in mitochondria), HSPs are reportedly expressed on the plasma membrane of different cancer types, such as ovarian cancer [49]. We do not yet know whether upregulation of HSPs (HSP27, HSP60, and HSP70) in TMEM102-overexpressing ovarian cancer cells only represents the increased malignant potential of these cells, or if TMEM102 directly interacts with HSPs. The Gene Ontolog (GO) annotation for TMEM102 indicates its mitochondrial location [50, 51]. Further research is needed to explore the mechanism of how TMEM102 inhibits apoptosis, and whether TMEM102 has a vital anti-apoptotic role or if its activity is regulated by other IAPs. Mitochondrial proteins, such as Smac/DIABLO, survivin, and cytochrome c, are released into the cytosol upon apoptotic stimulation [52, 53]. There remains a need for further studies to elucidate the possible complicated networks of the effects of TMEM102 in apoptosis pathways.

Our *in vitro* experiments showed that TMEM102 promotes chemoresistance in ovarian cancer cells through the upregulation of HSPs and survivin, and the inhibition of cytochrome c and caspase 9. In contrast to our findings, Kao *et al*. reported that TMEM102 plays a proapoptotic role via mitochondrial dysfunction in hematopoietic cell lines [19]. Further investigations of the biological functions and detailed pathways related to TMEM102 are warranted. Together, the above-described results suggest that TMEM102 exerts its anti-apoptotic role through a mitochondrial pathway, and that targeting TMEM102 is a promising therapeutic strategy for chemoresistant EOC.

Acknowledgements

This work was supported in part by the 7th core laboratory facility of the Department of Medical Research of National Taiwan University Hospital. This study was granted by the Ministry of Science and Technology of Taiwan (MOST 108-2314-B-002-061, MOST 109-2314-B-002-256, MOST 110-2314-B-002-274) and National Taiwan University Hospital (NTUH 108-M4195, 109-012, 109-M4598, 110-027). The funding agency had no role in study design, data collection and analysis, the decision to publish, or the preparation of the manuscript.

Disclosure of conflict of interest

None.

Address correspondence to: Wen-Fang Cheng, Department of Obstetrics and Gynecology, National Taiwan University Hospital, Taipei 100, Taiwan. Tel: 886-2-2312-3456 Ext. 71964; Fax: 886-2-2311-4965; E-mail: wenfangcheng@yahoo.com

References

[1] Taiwan Cancer Registry. Incidence and mortality rates for the top 10 cancer among females in Taiwan. 2018.

[2] Sung H, Ferlay J, Siegel RL, Laversanne M, Soerjomataram I, Jemal A and Bray F. Global cancer statistics 2020: GLOBOCAN estimates of incidence and mortality worldwide for 36 cancers in 185 countries. CA Cancer J Clin 2021; 71: 209-249.

[3] Gonzalez-Diego P, Lopez-Abente G, Pollan M and Ruiz M. Time trends in ovarian cancer mortality in Europe (1955-1993): effect of age, birth cohort and period of death. Eur J Cancer 2000; 36: 1816-1824.

[4] Chiang YC, Chen CA, Chiang CJ, Hsu TH, Lin MC, You SL, Cheng WF and Lai MS. Trends in incidence and survival outcome of epithelial ovarian cancer: 30-year national population-based registry in Taiwan. J Gynecol Oncol 2013; 24: 342-351.

[5] Marth C, Reimer D and Zeimet AG. Front-line therapy of advanced epithelial ovarian cancer: standard treatment. Ann Oncol 2017; 28: viii36-viii39.

[6] National Institute for Health and Care Excellence (NICE). (2017). Managing advanced (stage II-IV) ovarian cancer. London: NICE Pathways.

[7] Monk BJ, Minion LE and Coleman RL. Anti-angiogenic agents in ovarian cancer: past, present, and future. Ann Oncol 2016; 27 Suppl 1: i33-i39.

[8] Mirza MR, Monk BJ, Herrstedt J, Oza AM, Mahner S, Redondo A, Fabbro M, Ledermann JA, Lorusso D, Vergote I, Ben-Baruch NE, Marth C, Mądry R, Christensen RD, Berek JS, Dørum A, Tinker AV, du Bois A, González-Martín A, Follana P, Benigno B, Rosenberg P, Gilbert L, Rimel BJ, Buscema J, Balser JP, Agarwal S and Matulonis UA; ENGOT-OV16/NOVA Investigators. Niraparib maintenance therapy in platinum-sensitive, recurrent ovarian cancer. N Engl J Med 2016; 375: 2154-2164.

[9] Pujade-Lauraine E, Ledermann JA, Selle F, Gebski V, Penson RT, Oza AM, Jacob Korach J, Huzarski T, Poveda A, Pignata S, Friedlander M, Colombo N, Harter P, Fujiwara K, Ray-Coquard I, Banerjee S, Liu J, Lowe ES, Bloomfield R and Pautier P; SOLO2/ENGOT-Ov21 investigators. Olaparib tablets as maintenance therapy in patients with platinum-sensitive, relapsed ovarian cancer and a BRCA1/2 mutation (SOLO2/ENGOT-Ov21): a double-blind, randomised, placebo-controlled, phase 3 trial. Lancet Oncol 2017; 18: 1274-1284.

[10] Moore K, Colombo N, Scambia G, Kim BG, Oaknin A, Friedlander M, Lisyanskaya A, Floquet A, Leary A, Sonke GS, Gourley C, Banerjee S, Oza A, González-Martín A, Aghajanian C, Bradley W, Mathews C, Liu J, Lowe ES, Bloomfield R and DiSilvestro P. Maintenance olaparib in patients with newly diagnosed advanced ovarian cancer. N Engl J Med 2018; 379: 2495-2505.

[11] Perez RP, Hamilton TC, Ozols RF and Young RC. Mechanisms and modulation of resistance to chemotherapy in ovarian cancer. Cancer 1993; 71: 1571-1580.

[12] Norouzi-Barough L, Sarookhani MR, Sharifi M, Moghbelinejad S, Jangjoo S and Salehi R. Molecular mechanisms of drug resistance in ovarian cancer. J Cell Physiol 2018; 233: 4546-4562.

[13] Fletcher JI, Williams RT, Henderson MJ, Norris MD and Haber M. ABC transporters as mediators of drug resistance and contributors to cancer cell biology. Drug Resist. Updates; 2016. pp. 1-9.

[14] Damia G and Broggini M. Platinum resistance in ovarian cancer: role of DNA repair. Cancers (Basel) 2019; 11: 119.

[15] Mohammad RM, Muqbil I, Lowe L, Yedjou C, Hsu HY, Lin LT, Siegelin MD, Fimognari C, Kumar NB, Dou QP, Yang H, Samadi AK, Russo GL, Spagnuolo C, Ray SK, Chakrabarti M, Morre JD, Coley HM, Honoki K, Fujii H, Georgakilas AG, Amedei A, Niccolai E, Amin A, Ashraf SS, Helferich WG, Yang X, Boosani CS, Guha G, Bhakta D, Ciriolo MR, Aquilano K,

Chen S, Mohammed SI, Keith WN, Bilsland A, Halicka D, Nowsheen S and Azmi AS. Broad targeting of resistance to apoptosis in cancer. Semin Cancer Biol 2015; 35 Suppl: S78-S103.
[16] Ghoneum A, Almousa S, Warren B, Abdulfattah AY, Shu J, Abouelfadl H, Gonzalez D, Livingston C and Said N. Exploring the clinical value of tumor microenvironment in platinum-resistant ovarian cancer. Semin Cancer Biol 2021; 77: 83-98.
[17] Zou XQ, Zhao YJ, Liang XT, Wang H, Zhu YL and Shao QX. Double insurance for OC: miRNA-mediated platinum resistance and immune escape. Front Immunol 2021; 12: 641937.
[18] Zhan QL, Wang CM and Ngai SM. Ovarian cancer stem cells: a new target for cancer therapy. Biomed Res Int 2013; 2013: 916819.
[19] Kao CJ, Chiang YJ, Chen PH, Lin KR, Hwang PI, Yang-Yen HF and Yen JJ. CBAP interacts with the un-liganded common beta-subunit of the GM-CSF/IL-3/IL-5 receptor and induces apoptosis via mitochondrial dysfunction. Oncogene 2008; 27: 1397-1403.
[20] Ho KC, Chiang YJ, Lai AC, Liao NS, Chang YJ, Yang-Yen HF and Yen JJ. CBAP promotes thymocyte negative selection by facilitating T-cell receptor proximal signaling. Cell Death Dis 2014; 5: e1518.
[21] Chiang YJ, Ho KC, Sun CT, Chiu JJ, Lee FJ, Liao F, Yang-Yen HF and Yen JJ. CBAP functions as a novel component in chemokine-induced ZAP70-mediated T-cell adhesion and migration. PLoS One 2013; 8: e61761.
[22] Chiang YJ, Liao WT, Ho KC, Wang SH, Chen YG, Ho CL, Huang SF, Shih LY, Yang-Yen HF and Yen JJ. CBAP modulates Akt-dependent TSC2 phosphorylation to promote Rheb-mTORC1 signaling and growth of T-cell acute lymphoblastic leukemia. Oncogene 2019; 38: 1432-1447.
[23] Prat J; FIGO Committee on Gynecologic Oncology. Staging classification for cancer of the ovary, fallopian tube, and peritoneum. Int J Gynaecol Obstet 2014; 124: 1-5.
[24] Livak KJ and Schmittgen TD. Analysis of relative gene expression data using real-time quantitative PCR and the 2(-Delta Delta C(T)) method. Methods 2001; 25: 402-408.
[25] Chiang YC, Cheng WF, Chang MC, Lu TP, Kuo KT, Lin HP, Hsieh CY and Chen CA. Establishment of a new ovarian cancer cell line CA5171. Reprod Sci 2015; 22: 725-734.
[26] Hercus TR, Broughton SE, Ekert PG, Ramshaw HS, Perugini M, Grimbaldeston M, Woodcock JM, Thomas D, Pitson S, Hughes T, D'Andrea RJ, Parker MW and Lopez AF. The GM-CSF receptor family: mechanism of activation and implications for disease. Growth Factors 2012; 30: 63-75.
[27] Woodcock JM, Bagley CJ, Zacharakis B and Lopez AF. A single tyrosine residue in the membrane-proximal domain of the GM-CSF, IL-3 and IL-5 receptor common beta-chain is necessary and sufficient for high affinity binding and signaling by all three ligands. J Biol Chem 1996; 271: 25999-26006.
[28] Rossjohn J, McKinstry WJ, Woodcock JM, McClure BJ, Hercus TR, Parker MW, Lopez AF and Bagley CJ. Structure of the activation domain of the GM-CSF/IL-3/IL-5 receptor common b chain bound to an antagonist. Blood 2000; 95: 2491-2498.
[29] Bristow RE, Tomacruz RS, Armstrong DK, Trimble EL and Montz FJ. Survival effect of maximal cytoreductive surgery for advanced ovarian carcinoma during the platinum era: a meta-analysis. J Clin Oncol 2002; 20: 1248-1259.
[30] du Bois A, Reuss A, Pujade-Lauraine E, Harter P, Ray-Coquard I and Pfisterer J. Role of surgical outcome as prognostic factor in advanced epithelial ovarian cancer: a combined exploratory analysis of 3 prospectively randomized phase 3 multicenter trials: by the Arbeitsgemeinschaft Gynaekologische Onkologie Studiengruppe Ovarialkarzinom (AGO-OVAR) and the Groupe d'Investigateurs Nationaux Pour les Etudes des Cancers de l'Ovaire (GINECO). Cancer 2009; 115: 1234-1244.
[31] Pan ST, Li ZL, He ZX, Qiu JX and Zhou SF. Molecular mechanisms for tumour resistance to chemotherapy. Clin Exp Pharmacol Physiol 2016; 43: 723-737.
[32] Pihán P, Carreras-Sureda A and Hetz C. BCL-2 family: integrating stress responses at the ER to control cell demise. Cell Death Differ 2017; 24: 1478-1487.
[33] Bogner C, Kale J, Pogmore J, Chi X, Shamas-Din A, Fradin C, Leber B and Andrews DW. Allosteric regulation of BH3 proteins in Bcl-x(L) complexes enables switch-like activation of bax. Mol Cell 2020; 77: 901-912, e9.
[34] Llambi F and Green DR. Apoptosis and oncogenesis: give and take in the BCL-2 family. Curr Opin Genet Dev 2011; 21: 12-20.
[35] Marchion DC, Cottrill HM, Xiong Y, Chen N, Bicaku E, Fulp WJ, Bansal N, Chon HS, Stickles XB, Kamath SG, Hakam A, Li L, Su D, Moreno C, Judson PL, Berchuck A, Wenham RM, Apte SM, Gonzalez-Bosquet J, Bloom GC, Eschrich SA, Sebti S, Chen DT and Lancaster JM. BAD phosphorylation determines ovarian cancer chemosensitivity and patient survival. Clin Cancer Res 2011; 17: 6356-6366.
[36] Bansal N, Marchion DC, Bicaku E, Xiong Y, Chen N, Stickles XB, Sawah EA, Wenham RM, Apte SM, Gonzalez-Bosquet J, Judson PL, Hakam A and Lancaster JM. BCL2 antagonist of cell death kinases, phosphatases, and ovar-

ian cancer sensitivity to cisplatin. J Gynecol Oncol 2012; 23: 35-42.
[37] Zhou HM, Zhang JG, Zhang X and Li Q. Targeting cancer stem cells for reversing therapy resistance: mechanism, signaling, and prospective agents. Signal Transduct Target Ther 2021; 6: 62.
[38] Wheatley SP and Altieri DC. Survivin at a glance. J Cell Sci 2019; 132: jcs223826.
[39] He XY, Yang KH, Wang HL, Chen XH, Wu HF, Yao L and Ma SY. Expression and clinical significance of survivin in ovarian cancer: a meta-analysis. PLoS One 2018; 13: e0194463.
[40] Lu HY, Tai YJ, Chen YL, Chiang YC, Hsu HC and Cheng WF. Ovarian cancer risk score predicts chemo-response and outcome in epithelial ovarian carcinoma patients. J Gynecol Oncol 2021; 32: e18.
[41] Conway EM, Pollefeyt S, Steiner-Mosonyi M, Luo W, Devriese A, Lupu F, Bono F, Leducq N, Dol F, Schaeffer P, Collen D and Herbert JM. Deficiency of survivin in transgenic mice exacerbates Fas-induced apoptosis via mitochondrial pathways. Gastroenterology 2002; 123: 619-631.
[42] Altieri DC. Validating survivin as a cancer therapeutic target. Nat Rev Cancer 2003; 3: 46-54.
[43] Hoter A and Naim HY. Heat shock proteins and ovarian cancer: important roles and therapeutic opportunities. Cancers (Basel) 2019; 11: 1389.
[44] Garrido C, Brunet M, Didelot C, Zermati Y, Schmitt E and Kroemer G. Heat shock proteins 27 and 70: anti-apoptotic proteins with tumorigenic properties. Cell Cycle 2006; 5: 2592-2601.
[45] Arrigo AP and Gibert B. HspB1 dynamic phospho-oligomeric structure dependent interactome as cancer therapeutic target. Curr Mol Med 2012; 12: 1151-1163.
[46] Yin L, Yang YH, Zhu WL, Xian Y, Han ZY, Huang HY, Peng LT, Zhang K and Zhao Y. Heat shock protein 90 triggers multi-drug resistance of ovarian cancer via AKT/GSK3beta/beta-catenin signaling. Front Oncol 2021; 11: 620907.
[47] Calderwood SK, Khaleque MA, Sawyer DB and Ciocca DR. Heat shock proteins in cancer: chaperones of tumorigenesis. Trends Biochem Sci 2006; 31: 164-172.
[48] Shevtsov M, Balogi Z, Khachatryan W, Gao H, Vígh L and Multhoff G. Membrane-associated heat shock proteins in oncology: from basic research to new theranostic targets. Cells 2020; 9: 1263.
[49] Shin BK, Wang H, Yim AM, Le Naour F, Brichory F, Jang JH, Zhao R, Puravs E, Tra J, Michael CW, Misek DE and Hanash SM. Global profiling of the cell surface proteome of cancer cells uncovers an abundance of proteins with chaperone function. J Biol Chem 2003; 278: 7607-7616.
[50] Ashburner M, Ball CA, Blake JA, Botstein D, Butler H, Cherry JM, Davis AP, Dolinski K, Dwight SS, Eppig JT, Harris MA, Hill DP, Issel-Tarver L, Kasarskis A, Lewis S, Matese JC, Richardson JE, Ringwald M, Rubin GM and Sherlock G. Gene ontology: tool for the unification of biology. The Gene Ontology Consortium. Nat Genet 2000; 25: 25-29.
[51] Gene Ontology Consortium. The Gene Ontology resource: enriching a GOld mine. Nucleic Acids Res 2021; 49: D325-D334.
[52] Dohi T, Beltrami E, Wall NR, Plescia J and Altieri DC. Mitochondrial survivin inhibits apoptosis and promotes tumorigenesis. J Clin Invest 2004; 114: 1117-1127.
[53] Song ZY, Yao XB and Wu M. Direct interaction between survivin and Smac/DIABLO is essential for the anti-apoptotic activity of survivin during taxol-induced apoptosis. J Biol Chem 2003; 278: 23130-23140.

Supplementary Table 1. Mean expression levels of TMEM102 and its correlation with clinicopathologic factors

	TMEM102 expression level* Mean ± SD	P
FIGO stage		
Early	0.023±0.005	0.014*
Advanced	0.046±0.005	
Tumor grade		
Low (I/II)	0.023±0.003	0.005*
High (III)	0.057±0.007	
Lymph node metastasis		
No	0.030±0.006	0.092
Yes	0.035±0.007	
Chemotherapy response		
Platinum-sensitive	0.034±0.004	0.022*
Platinum-resistant	0.057±0.010	
Recurrence or progression		
No	0.016±0.002	0.012*
Yes	0.054±0.006	
Outcome		
Alive	0.034±0.005	0.045*
Dead	0.053±0.007	

*The expression level was calculated using the 2-ΔΔCt method. *P*-value by Mann-Whitney U test.

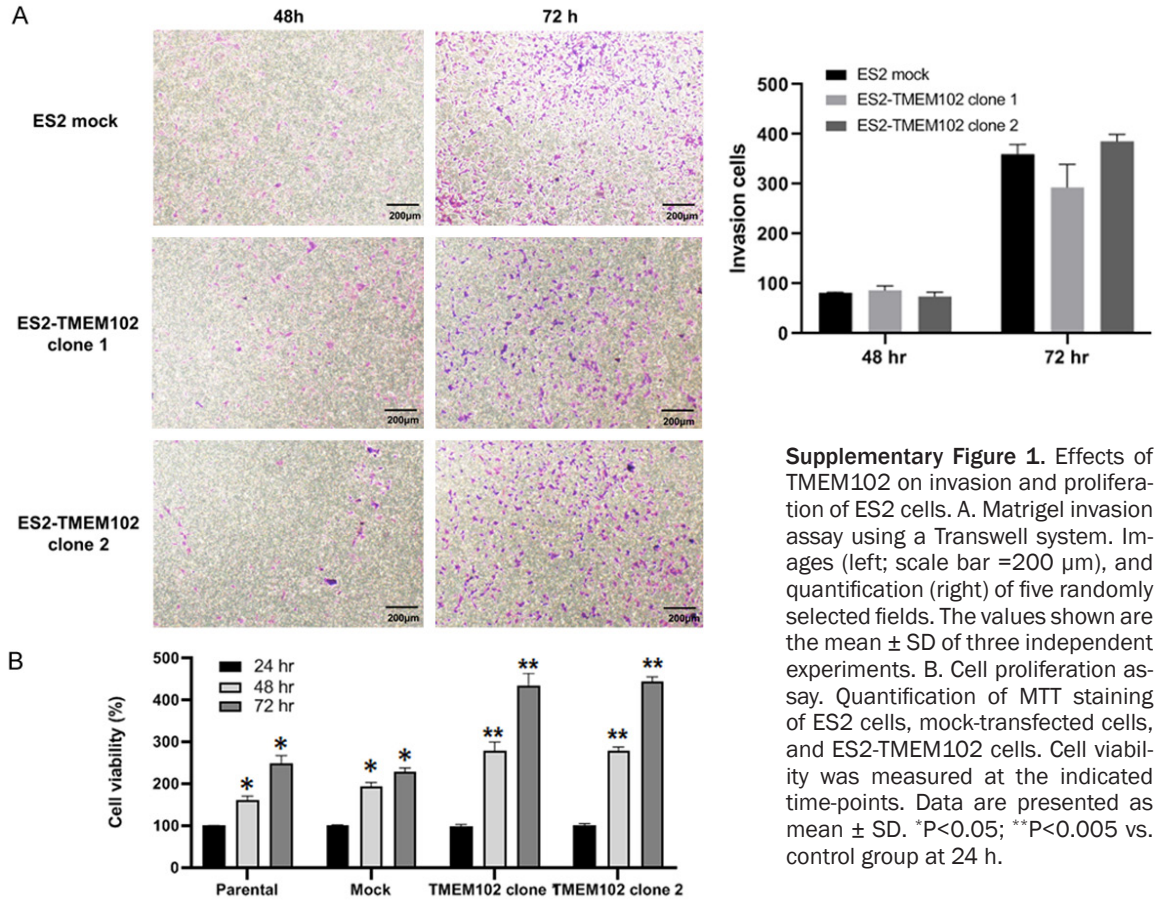

Supplementary Figure 1. Effects of TMEM102 on invasion and proliferation of ES2 cells. A. Matrigel invasion assay using a Transwell system. Images (left; scale bar =200 μm), and quantification (right) of five randomly selected fields. The values shown are the mean ± SD of three independent experiments. B. Cell proliferation assay. Quantification of MTT staining of ES2 cells, mock-transfected cells, and ES2-TMEM102 cells. Cell viability was measured at the indicated time-points. Data are presented as mean ± SD. *P<0.05; **P<0.005 vs. control group at 24 h.